



# The Arctic tern *Sterna paradisaea*: consistency and variability in spatial use at a global oceanographic scale

Chris P. F. Redfern<sup>1,2,\*</sup>, Richard M. Bevan<sup>1</sup>

<sup>1</sup>School of Natural & Environmental Sciences, Newcastle University, Newcastle Upon Tyne NE2 4HH, UK

<sup>2</sup>Natural History Society of Northumbria, Great North Museum: Hancock, Newcastle Upon Tyne NE2 4PT, UK

**ABSTRACT:** Elucidating the ecological factors underpinning migratory strategies of seabirds is necessary for understanding resilience to environmental change. Arctic terns *Sterna paradisaea* breed in the Northern Hemisphere and are unique for the global scale of their migration. Geolocator data from 37 Arctic terns breeding in a low-latitude colony, 10 of which were re-tagged in successive years, were analysed to characterise their migratory behaviour and to test the hypothesis that individuals have repeatable migration strategies. Seawater immersion data suggested a fly–forage strategy, with birds remaining on the wing at night and only foraging during daylight. Southward movement was focused initially along Atlantic eastern-boundary upwelling systems. Most terns then reoriented eastwards, crossing the southern Indian Ocean before moving south to the Antarctic. Foraging intensity differed between migration phases. Indian Ocean foraging locations were diverse, and less frequent over deep ocean basins. Foraging intensity was highest in the later stages of return migration, particularly in and around the Azores Confluence Zone. High movement speeds and foraging intensity on return migration may be adaptations to optimise reproductive success. Some aspects of migration phenology were repeatable between years, but trajectories were displaced by wind. Repeat birds did not use the same foraging areas in different years, and their trajectories across the Indian Ocean also differed. The results of this study suggest that the Indian Ocean crossing is a behaviour pattern, surviving since the last ice age, enabling Arctic terns breeding at low-latitude northwest European colonies to arrive at fragmenting Antarctic sea ice when foraging conditions are suitable.

**KEY WORDS:** Arctic tern · Indian Ocean · Thermal fronts · Sea surface height · Chlorophyll · Foraging · Migration speed · Geolocator

—Resale or republication not permitted without written consent of the publisher—

## 1. INTRODUCTION

For true migrants, the advantages of migrating between breeding and non-breeding areas must be greater than remaining in the breeding environment (Hedenström 2008). Flight enables birds to sustain rapid movement over large distances to areas where predictable foraging resources can be exploited. Migratory species are each defined by a suite of physical and behavioural adaptations (Åkesson &

Hedenström 2007). Physical and physiological adaptations to flight demands are well known (Butler 2016, Vágási et al. 2016), but behavioural adaptations underlying the evolution of migration patterns are less clear. Key factors are the degree to which individuals adjust migration routes and timing in response to environmental conditions, and the extent of interspecific variation in adapting to changing environments along the way (Åkesson & Helm 2020). The ability to adapt to unpredictable foraging resources

\*Corresponding author: chris.redfern@newcastle.ac.uk

can be an important component of a successful migration strategy, but also may carry unexpected costs for breeding success (Fayet et al. 2017).

The Arctic tern *Sterna paradisaea* is a migratory Northern Hemisphere breeding species with a circumpolar breeding distribution extending over a 35° range of latitudes, from 45° on the northwest Atlantic coast to >80° in Svalbard. At high latitudes, breeding is constrained into a narrow window between the seasonal disappearance and return of snow cover which, at least in the decades before the acceleration of global warming (Killie et al. 2021), may be only just sufficient time to raise chicks to fledging. Conversely, those breeding further south have greater flexibility in the timing of breeding.

Arctic terns spend at least a third of their annual cycle exploiting foraging resources associated with sea ice in the Antarctic, a habitat to which they seem to be, amongst the terns, uniquely adapted (Redfern & Bevan 2020b). Their twice-yearly movement between the Northern Hemisphere and Antarctic non-breeding areas entails a near pole-to-pole migration (Egevang et al. 2010, Fijn et al. 2013, Alerstam et al. 2019, Hromádková et al. 2020, Redfern & Bevan 2020b, Redfern 2021). The global scale of Arctic tern migration is almost unique amongst vertebrates and raises questions about the evolution of this migratory strategy and the behavioural adaptations on which it is based.

While in the Antarctic, Arctic terns undergo a complete moult, which may restrict flight ability (Cline et al. 1969, Voelker 1997). As in many species, the constraints of breeding and moulting, stages in the avian annual cycle with restrictions on mobility, have implications for the scheduling of migration (Hedenström 2008). Furthermore, foraging in the Antarctic will be dependent upon the availability of prey associated with fragmenting sea ice (Redfern & Bevan 2020b), and progression of the austral spring and summer on which sea-ice fragmentation depends may be an additional constraint on migration strategies.

Arctic terns from Greenland, Alaska, Iceland and Svalbard (Egevang et al. 2010, Duffy et al. 2014, Hromádková et al. 2020) enter the Antarctic predominantly via the Weddell Sea. Conversely, those from northwest European colonies, mainly bordering the North Sea, tend to enter the Antarctic much further east after crossing the southern Indian Ocean (Fijn et al. 2013, Alerstam et al. 2019, Redfern & Bevan 2020b, Redfern 2021). Longitudes of entry into the Antarctic show some repeatability within individuals in subsequent seasons (Redfern & Bevan 2020b), implying that individuals might also follow repeat-

able trajectories across the Indian Ocean, linked by foraging resources to their Antarctic entry points. Once in the East Antarctic, Arctic terns from North Sea colonies move west during the austral summer and early autumn, with most birds departing from the Antarctic Southern Ocean directly into the South Atlantic (Redfern & Bevan 2020b).

While we now have a better understanding of the importance of Antarctic sea ice as a foraging environment of Arctic terns (Redfern & Bevan 2020b), their behaviours and use of oceanic resources during their extensive migration before arrival in the Antarctic are not well understood. Characterising the outward and return migration phases of Arctic terns and how these might differ between geographically distinct breeding populations is crucial for understanding the evolution of migratory strategies and the potential effects of changes in climate and ocean productivity. The aim of this study was to use geolocator data to characterise the behaviour and activities of Arctic terns on migration from a North Sea breeding colony to test the hypothesis that individual Arctic terns show repeatable behaviour with respect to their migratory routes and foraging locations, and to understand the reason for different behaviour patterns by birds from different breeding latitudes.

## 2. MATERIALS AND METHODS

### 2.1. Breeding site and geolocators

Arctic terns nesting on Inner Farne, Farne Islands, UK (decimal degrees: longitude -1.656; latitude 55.617) were trapped on the nest and fitted with Inti-geo-W65A9-SEA geolocators (Migrate Technology) in 2015 (27 birds) and 2017 (25 birds). The geolocators were mounted on plastic leg rings and weighed ~0.95 g (<1% of body mass; Redfern & Bevan 2020a,b). There was no evidence for detrimental effects on the birds (see supplement in Redfern 2021). Most devices were recovered the following year: 21 from the 2015 group and 24 from the 2017 group, but 3 from 2015 were recovered after 2 yr (2 devices) and 4 yr (1 device), an overall retrieval rate of 89% and 96% for the 2 groups, respectively. Repeatability of migration behaviour was studied by retagging 11 individuals (referred to as repeat birds) from the 2015 cohort with new geolocators in 2017; one did not return in 2018 or in subsequent years. For the remaining 10 sets of repeat data, the geolocator for one of the birds in the 2015 cohort had failed part-way through the 2015–2016 winter; therefore, there

were 10 sets of repeat data for outward (autumn) migration and 9 for the return (spring) migration. The study was carried out under a permit issued by the British Trust for Ornithology with endorsement permitting the use of leg-ring mounted geolocators.

Light levels recorded by the geolocators were interpreted to define dawn and dusk and used to derive position. Conductivity, seawater immersion state and maximum/minimum temperatures were also recorded. All devices in the 2017 group and half in the 2015 group were programmed to record full light levels, seawater immersion state (defined by conductivity threshold) measured as every 30 s interval with at least 1 instantaneous immersion event per 4 h period (giving a theoretical maximum count of 480), and conductivity and minimum and maximum temperature every 4 h. The remaining devices in the 2015 group were programmed to record in 'clipped' light level mode, with seawater immersion counts (every 30 s period with an immersion event) and conductivity recorded every 10 min. Immersion counts for 1 geolocator were discounted because the maximum or near-maximum counts recorded throughout the annual cycle were not consistent with inferred location and movement data and indicate that the immersion sensor was not working correctly (Fig. S1 in the Supplement at [www.int-res.com/articles/suppl/m691p151\\_suppl.pdf](http://www.int-res.com/articles/suppl/m691p151_suppl.pdf)).

## 2.2. Data processing and data sources

Data were analysed using R v.3.6.1 (R Core Team 2019). *FLightR* (Rakhimberdiev et al. 2015, 2017) was used to estimate longitude and latitude at dawn/dusk twilight thresholds (Redfern & Bevan 2020a,b, Redfern 2021). Longitude and latitude coordinates are expressed as decimal degrees on a number line centred on the Greenwich Meridian ( $x = 0$ ) and the Equator ( $y = 0$ ). An average location accuracy of 50 km was assumed (Rakhimberdiev et al. 2016). Stationary periods of 2 or more days were estimated by *FLightR* as periods with movements between twilight intervals of <45 km (Rakhimberdiev et al. 2015). The median 'datetimes' of entry and exit from *FLightR* stationary periods were used to assign behavioural classifications of 'stationary', or, outside these periods, as 'moving', to geolocations and geolocation intervals. Intervals were assigned as day (dawn to dusk) or night (dusk to dawn). Distance (m) between coordinates, location of interval mid-points and forward bearings were calculated using the *distHaversine*, *midpoint* and *bearing* functions of the R pack-

age *geosphere* (Hijmans et al. 2019). Location-to-location interval speeds ( $\text{m s}^{-1}$ ) were distances divided by threshold-to-threshold time intervals (s). To estimate flow assistance from tailwinds (negative tailwinds are headwinds) at interval midpoints, the function *NCEP.Tailwind* from the R package *RNCEP* (Kemp et al. 2012) was used, together with  $u$  (west-east) and  $v$  (south-north) wind vectors, derived using the *rWind* package (Fernández-López & Schliep 2019); wind heights were 10 m above sea level. Immersion counts per complete 4 h period that did not overlap dawn or dusk thresholds were assigned to day or night and the mean 4 h immersion count per day or night interval calculated. For those geolocators from the 2015 group that stored immersion counts every 10 min, these counts were combined to 4 h periods and the means per 4 h period in day or night intervals calculated.

Boundaries or fronts between water masses, arising from upwellings and eddies, are drivers of marine productivity (Woodson & Litvin 2015) and can be detected by sharp gradients in properties such as sea surface temperature (SST), sea surface height anomalies (SSH) and chlorophyll *a* (chl *a*) concentrations (Belkin 2021). Satellite data for chl *a* and SST were monthly Level 3 Standard Mapped Image Modis-Aqua OceanColor data at 4 km resolution (<https://oceandata.sci.gsfc.nasa.gov/MODIS-Aqua>); gridded ( $1/6^{\text{th}}$  degree grid) SSH data were from [https://podaac-opendap.jpl.nasa.gov/opendap/allData/merged\\_alt/L4/cdr\\_grid](https://podaac-opendap.jpl.nasa.gov/opendap/allData/merged_alt/L4/cdr_grid) and averaged to monthly periods for compatibility with chl *a* and SST data. Rasters for ocean fronts, reflecting high rates of change in chl *a* concentrations (log scale; ratio values for gradient intensity), SST ( $^{\circ}\text{C km}^{-1}$ ) and SSH (gradient intensity, unitless), were calculated (Belkin & O'Reilly 2009) from chl *a*, SST and SSH data using the *detect-Fronts* function of the R package *grec*. These rasters, transformed to Albers Equal Area Conic projections, were used to calculate mean gradient intensities within a 50 km radius of geolocation points. Chl *a* concentrations (log scale) at geolocation points were also averaged within a 50 km radius for separate analyses. High-resolution bathymetric data (15 arc-second intervals) were from the GEBCO\_2021 Grid (GEBCO Bathymetric Compilation Group 2021) and reduced to a 10-fold lower resolution for analysis.

## 2.3. Behaviour on migration

For analysis of migration routes, we considered the core of the migratory cycle between the UK and the

Antarctic as 2 outward stages and 1 return stage: southward migration through the Atlantic Ocean from 50° to the southern tip of Africa (Cape Agulhas), easterly movement across the Indian Ocean (and to the Pacific Ocean for some birds), and return migration north from the Antarctic through the Atlantic to the UK. After leaving the Farne Islands, geolocator-tagged Arctic terns cross the UK to the Irish Sea, where, in some years, they may remain for a while before initiating migration further south (Redfern & Bevan 2020a). We defined the initiation of outward migration in terms of the date (day of the year) at which consistent movement south from the British Isles was initiated. For most birds, this was apparent as movement past 50°, but for some birds, southerly movement was initiated from further north, and for these birds the date of departure was defined on the basis of change-point analysis on latitude.

The day of the year at which the Indian Ocean phase started and ended for each bird was based on change-point analysis of change in longitude and in latitude, respectively, using the R package *change-point* (Killick et al. 2012), function *cpt.meanvar* with the PELT algorithm, Schwarz information criterion penalty and minimum segment length 3. For most birds, the change from a southward to eastward trajectory (start of the Indian Ocean phase) or an eastward to a southward trajectory (end of the Indian Ocean phase) was abrupt and easy to define objectively on the basis of change points, but for some, the transition was more gradual and required subjective interpretation to define a transition point. We did not include the movement south from the Indian Ocean to Antarctica in our analysis of migration because, in this short phase, birds enter a sea-ice zone (Redfern & Bevan 2020b) where movement and behaviour may be determined by sea-ice melt and fragmentation, conditions not applicable to other migration phases.

For return migration, dates of departure from Antarctica were defined by minimum temperature readings and were reported previously (Redfern & Bevan 2020b). The end of the return migration phase was defined by movement past 50° latitude. All phenology measures were defined in the first stage of data analysis and remained fixed thereafter.

Although we regarded the core of the migratory cycle as 2 outward and 1 return phase, the data for return migration (see Fig. 1) suggested behavioural differences between the early and later parts of this phase. Therefore, for comparing behaviour between the different migration phases, we separated the return phase at latitude 15° (see Fig. 1b) into 2 parts: Return-a, the first part from the Antarctic, and

Return-b, the last part before arrival at 50°. Behaviour in these 4 phases (Atlantic outward, Indian Ocean, Return-a and Return-b) was then compared using seawater immersion counts and interval speeds as dependent variables. Chl *a* and ocean fronts at bird geolocations were also compared across migration phases in separate analyses. Data for 5 birds in the 2015 cohort which had geolocators that failed before return migration and for 1 bird from the 2017 cohort which had erroneous immersion data readings were excluded from this analysis. Data for birds that were tagged twice, once in 2015 and again in 2017, were regarded as independent between years in behaviour analyses.

## 2.4. Statistical methods

Phenology dates were compared between year group by *t*-tests after correction of leptokurtosis or skew by Lambert W transformation (R package *LambertW*: Goerg 2011, 2020). Repeatability of phenology dates and longitudes for repeat birds was tested using the R package *rptR* (Stoffel et al. 2017).

Dependent behaviour variables (interval speed and seawater immersion counts) were analysed in generalised linear mixed-effects models (GLMMs) using the R package *glmmTMB* (Brooks et al. 2017) or *lme4* (Bates et al. 2015). Seawater immersion counts were transformed to a beta distribution (interval 0, <1; division of counts by 481) for use as a dependent variable and analysed using *glmmTMB* with a beta family distribution in zero-inflation models with zero inflation as random effect terms per bird (ID) in interaction with interval type (day/night) and ID in interaction with migration phase. For GLMMs with interval speeds, gamma-family distributions (log link) were used. In GLMMs for seawater immersion counts or interval speeds, independent variables (fixed effects) were migration phase, chl *a*, tailwinds and mean wind speeds, interval type (day, night), year cohort (2015 or 2017), seawater immersion counts (for interval speed GLMMs) and geolocation behaviour classification ('moving' or 'stationary'); continuous fixed effects were scaled to mean = 0 and SD = 1. Different random effects investigated in models were ID, migration phase or interval type (day/night) per ID, ID and interaction with interval type, migration phase, or cohort. Model selection was via Akaike's information criterion (AIC). The *lsmeans* and *emmeans* R packages (Lenth 2019) were used to extract main and interaction effects, and least-squared means contrasts for fixed effects, from the best-supported models. Contributions

of fixed effects in models were assessed by analysis of deviance, type III tests, with the R package *car* (Fox & Weisberg 2011).

For chl *a* at bird locations, normalised by Box-Cox transformation, a linear mixed-effects model was used with the interaction between ID and migration phase as a random effect; the top model had migration phase and geolocation behaviour classification as fixed effects with interaction. GLMMs with a gamma-family distribution, inverse link function, and bird ID as a random effect were used for analysis of mean rates of change (ocean fronts) of chl *a*, SST or SSH within 50 km radius of geolocation points (dependent variables), with migration phase, behaviour ('stationary or 'moving') and year group as independent predictors; rows with no satellite data were removed. In these analyses, the full interaction model (migration phase \* behaviour \* year group) was the top model for all ocean-front types. For the ocean front data, there was a high correlation between chl *a* and SST (current data: correlation coefficient,  $r = 0.28$ ;  $p < 0.001$ ), SST and SSH ( $r = 0.55$ ,  $p < 0.001$ ; see also Jones et al. 1998), but not between SSH and chl *a* ( $r = 0.02$ ;  $p = 0.09$ ).

For graphic interpretation of tailwind data in each migration phase, GLMM additive models were fitted to the data (R package *mgcv*), with ID as a random effect (Wood 2011). Robust linear mixed-effects models (RLMM) using the *robustlmm* R package (Koller 2016) were used to compare longitudes and wind vectors for the early part of return migration.

Stationary-period geolocations were assessed in relation to Indian Ocean bathymetry using a binomial GLMM with mean depth (within 50 km radius of geolocations) of  $>3000$  m = 1, or 0 otherwise; geolocation status (moving or stationary) was the independent variable and bird ID the random effect (R package *lme4*). In addition, a GLM was used to compare depth (continuous dependent variable) at moving and stationary-period geolocations. The data for these bathymetric analyses included data from 2 of the 2015 geolocators recovered after more than a year which had each yielded data for an additional outward migration across the Indian Ocean.

### 3. RESULTS

#### 3.1. Migration between a North Sea breeding colony and the Antarctic

Data from the 48 geolocators indicated that birds initially travelled south from the Irish Sea and the

North Atlantic west of Ireland, becoming focused in a relatively narrow corridor in the east Atlantic off Guinea to Liberia, before broadening out across the Gulf of Guinea, with some birds taking a direct route to the Angolan/Namibian coast and others diverting into the Gulf and taking a more coastal route from Gabon southwards (Fig. 1). Movement was then concentrated along the west coast of Africa from Equatorial Guinea south to the Benguela Current (BC) from Angola to Cape Agulhas of South Africa. Four birds departed from this pattern by moving westwards along the line of the subsea Walvis Ridge towards the central South Atlantic; one of these birds (ID G09, tagged in 2015) roamed within the central South Atlantic before continuing south to the Antarctic near the Weddell Sea (Fig. 1). The other 3, along with the rest of the tagged birds, changed orientation within latitudes  $-35^\circ$  to  $-40^\circ$  from predominantly southward to eastward. This change in orientation, which occurred at longitudes  $22^\circ$ ,  $-10^\circ$  and  $3^\circ$  for the 3 birds (G44-2017, G57-2015 and G60-2017, respectively) that had moved west into the South Atlantic, and between  $7^\circ$  and  $41^\circ$  (mean:  $24^\circ$ ) for the others, marked the start of an extensive movement east across the Indian Ocean. G60 was a repeat bird, also tagged in 2015, and in that year did not move west towards the central South Atlantic.

The birds travelled east across the Indian Ocean within a  $20$ – $30^\circ$  range of latitudes (Fig. 1), with 7 reaching the Pacific Ocean. At different points along this eastward trajectory, orientation changed again to predominantly southward, marking the end of the Indian Ocean traverse, and the birds approached the East Antarctic coastline in 3 broad streams, arriving, respectively, between longitudes  $50^\circ$ – $120^\circ$  (Enderby Land to Wilkes Land; 25 birds),  $120^\circ$ – $170^\circ$  (Wilkes Land to Oates Land; 16 birds), and some further east to the Ross Sea area (6 birds; Fig. 1).

Compared to outward migration, the northward return migration through the Atlantic was more direct, at an individual level and less focused for the tagged birds as a group, with the routes of some birds extending much further west almost to the South American coastline. Many appeared to follow great-circle routes through the Atlantic from the southern end of the South Atlantic to Senegal latitudes (Fig. 1). Some then changed orientation and followed a great-circle route back to the UK, but most continued north to between latitudes  $40^\circ$  or  $45^\circ$  before turning northeast towards the breeding colony.

The scale of Arctic tern migration through the Atlantic entailed movement across global atmospheric



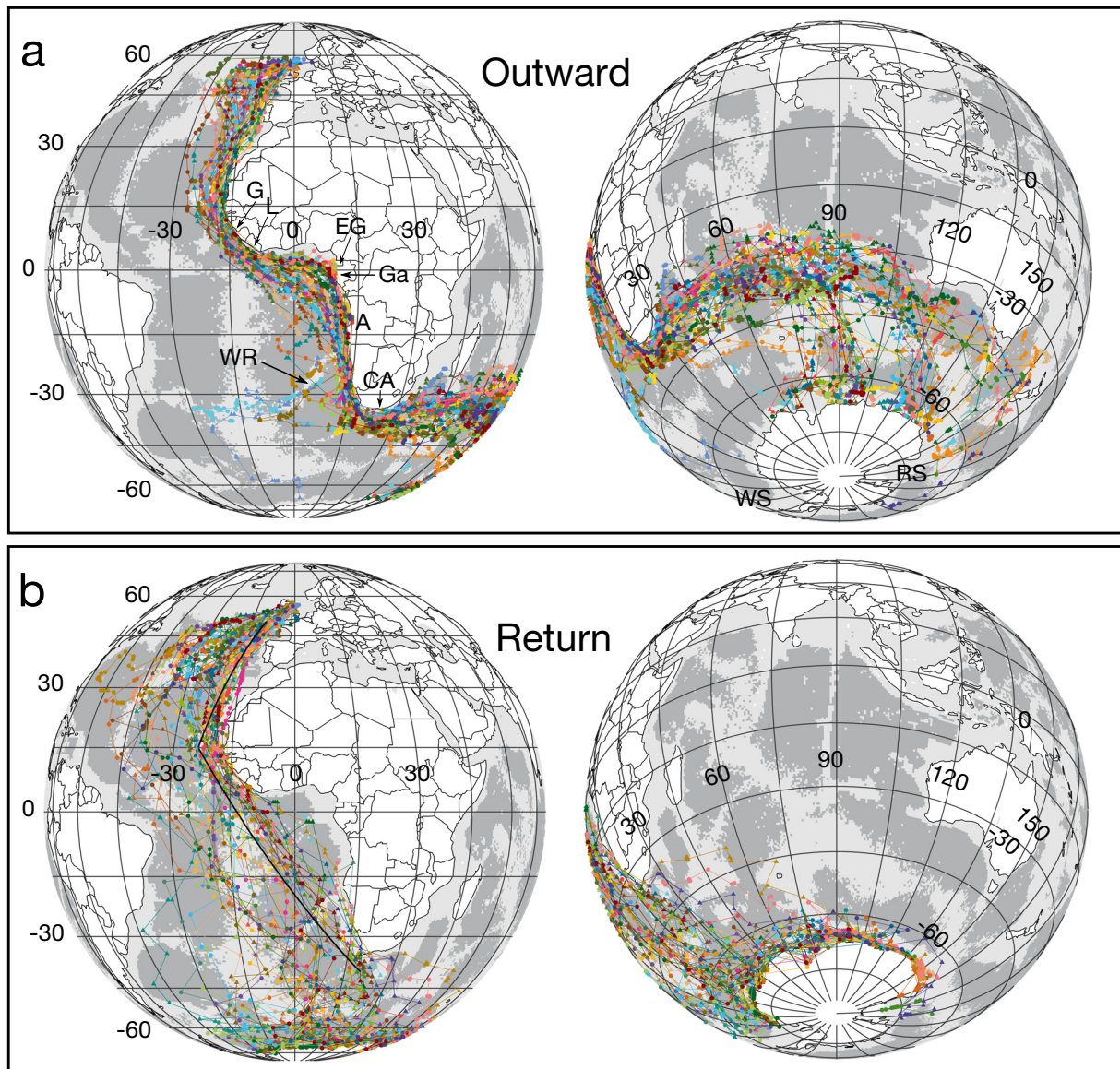


Fig. 1. Geolocator positions from 24 Arctic terns tagged in 2015 (filled triangles) and 24 tagged in 2017 (filled circles) plotted on global orthographic projections showing coastlines and ocean bathymetry (dark grey: depths >4000 m; light grey: depths <4000 m; white: above sea level). Two orientations shown for (a) outward migration and (b) return migration the following year; points linked by lines to indicate temporal relationships between successive geolocations. Within year, each bird is indicated by a different colour. Location positions: median longitude and latitudes determined using *FLightR*; data for 24 h day-light periods in Redfern & Bevan (2020b). Black lines in panel b (left) plotted from longitude of Cape Agulhas (CA; South Africa) at latitude  $-40^\circ$ , to the North Atlantic at longitude  $-23.5^\circ$ , latitude  $15^\circ$ , and from there to longitude  $-10^\circ$ , latitude  $50^\circ$ , show the shortest great circle routes between these points. WR: Walvis Ridge; G: Guinea; L: Liberia; EG: Equatorial Guinea; Ga: Gabon; A: Angola; WS: Weddell Sea; RS: Ross Sea

circulation bands, with tailwinds which varied in strength by latitude from strongly negative (headwinds) to positive during the southward and northward (return) migrations (Fig. 2). In contrast, tailwinds remained, on average, weakly positive during the entire eastward Indian Ocean phase (Fig. 2).

### 3.2. Phenology of outward migration

Mean departure from the British Isles was a week later in 2017 compared to the 2015 group ( $t = -3.04$ ,  $df = 45.8$ ,  $p = 0.004$ ), but was repeatable for birds tagged in both years (Table 1). The start of the Indian Ocean traverse occurred at similar dates (mean,

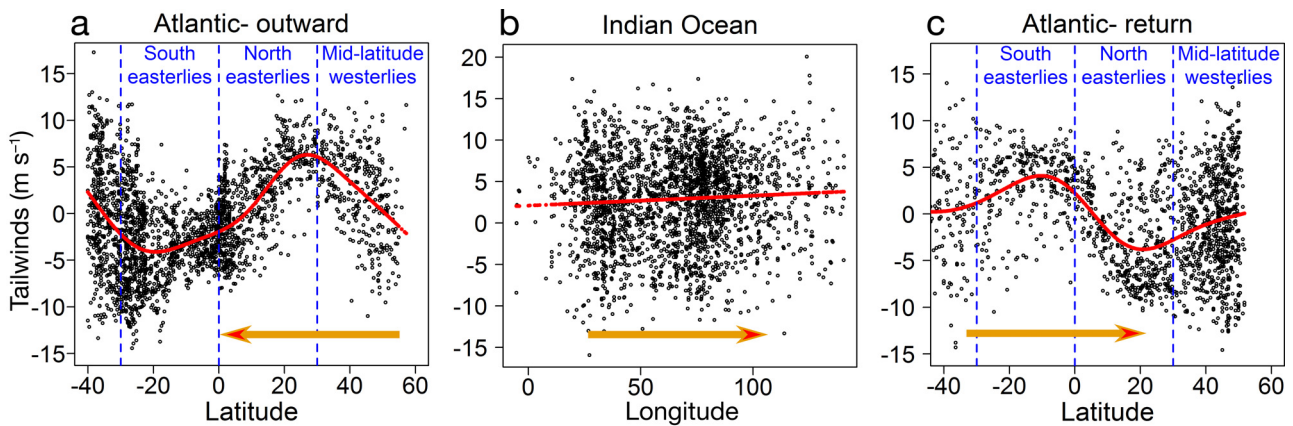


Fig. 2. Tailwind speeds (ordinate; headwinds are negative) at (a,c) location latitudes (abscissa), or (b) longitude, for all tagged Arctic terns (open circles) with interval speeds  $>0$ , at (a) the Atlantic phase and (b) Indian Ocean phase of autumn migration, and (c) the northward return migration through the Atlantic in spring. Red lines: generalised mixed-effects additive models fitted to the data, with individual bird as a random effect; vertical dotted blue lines: latitudinal Hadley (south- and northeasterlies) and mid-latitude atmospheric circulation cell boundaries; orange arrows: direction of bird movement

Table 1. Migration phenology of tagged Arctic terns and repeatability by re-tagged individuals. Mean day is day of the year, rounded to nearest day, followed by date. In 'Difference probability': n is sample size in 2015 group/2017 group

Event	Mean day; 2015 group (median; range)	Mean day; 2017 group (median; range)	Difference probability	Repeatability
Departure from British Isles latitude 50° N	212: 31 July (209; 203–226)	219: 7 August (220; 201–244)	0.004; n = 24/24	Yes; R = 0.587, n = 10, p = 0.02
Transition to Indian Ocean traverse	262: 19 September (265; 238–291)	263: 20 September (266; 240–281)	$>0.65$ ; n = 23/24	No <sup>a</sup> ; n = 10, p = 1
End of Indian Ocean traverse	307: 3 November (307; 285–332)	307: 3 November (308; 293–320)	$>0.8$ ; n = 23/24	Yes <sup>b</sup> ; R = 0.615, n = 10, p = 0.015
Departure from Antarctic: start of Atlantic return	87: 27 March (87; 71–103)	87: 28 March (88; 76–97)	0.8; n = 20/24	No; n = 9, p = 0.5
Arrival at British Isles latitude 50° N	124: 3 May (124; 118–142)	126: 6 May (126; 110–167)	$>0.11$ ; n = 19/24	No; n = 9, p = 0.5

<sup>a</sup>No repeatability in longitudes at transition, p = 0.5; <sup>b</sup>Longitudes at end of Indian Ocean traverse were also repeatable, n = 10, R = 0.755, p = 0.002, but not latitudes: R = 0.354, p = 0.124

19–20 September) in both years, but there was no indication for repeatability by individuals either in timing or longitude (Table 1). The date at which the Indian Ocean traverse ended and birds made the transition to a southward movement also did not differ between year groups ( $p > 0.8$ ; Table 1) and was repeatable for the 10 retagged individuals. The longitudes, but not latitudes, at transition were also repeatable (Table 1). For all birds, the latitudes at transition were  $\geq 5^\circ$  north of the Antarctic Polar Front (Fig. S2). On average, the Indian Ocean phase lasted 44 d.

### 3.3. Behaviour during migration

We tested the hypothesis that resource use and behaviour by the birds differed between the 4 migra-

tion phases, Atlantic outward, Indian Ocean, and with the northward return migration separated into Return-a and Return-b phases (see Section 2.3), using geolocation interval speeds and seawater immersion frequencies in relation to environmental and oceanographic characteristics.

Given varying night/day length, interval speed ( $\text{m s}^{-1}$ ), rather than distance travelled, is the most appropriate measure to compare night and daytime (interval type) movement. For geolocation intervals where interval speeds were positive ( $>0$ ), the best GLMM predicting interval speed had, as separate random effects, individual bird (ID) as an interaction with migration phase and ID as an interaction with interval type. In this model, interval speeds differed by day and night (analysis of deviance:  $\chi^2 = 10.13$ ,  $\text{df} = 1$ ,  $p = 0.001$ ), migration phase ( $\chi^2 = 126.7$ ,  $\text{df} = 3$ ,

$p < 0.001$ ; Fig. 3a), seawater immersion counts ( $\chi^2 = 9.21$ ,  $df = 1$ ,  $p < 0.01$ ) and tailwind (as a second-order term,  $\chi^2 = 16.93$ ,  $df = 2$ ,  $p < 0.001$ ; Table S1). Interval speeds increased in relation to tailwind and decreased in relation to seawater immersion (Fig. 3b,c). Year of tagging was not significant as a main effect ( $\chi^2 = 0.025$ ,  $df = 1$ ,  $p = 0.87$ ). Migration phases differed with respect to interval speeds, averaged by tailwind, year and interval type. Mean speeds on the first phase of return migration (Return-a) were considerably higher than for other phases (least-squares mean pairwise contrast,  $|t| > 6$ ,  $df = 6506$ ,  $p < 0.001$ ); mean interval speed on the latter part of return migration (Return-b) was also higher than in the Atlantic outward and Indian Ocean phases ( $|t| > 2.7$ ,  $df = 6506$ ,  $p < 0.01$ ). Although mean interval speed during the Atlantic outward phase was higher than during the Indian Ocean traverse ( $t > 2.9$ ,  $df = 6506$ ,  $p = 0.004$ ), this was a result of significantly lower interval speeds at night compared to during the day in the Indian Ocean (Fig. 3a;  $t = 2.75$ ,  $df = 6506$ ,  $p = 0.006$ ) and otherwise daytime interval speeds were

similar. Within the other migration phases, mean interval speeds were similar for day and night geolocation intervals ( $|t| < 0.33$ ,  $df = 6506$ ,  $p \geq 0.75$ ; Fig. 3a).

From the distribution of seawater immersion counts (Fig. S1), there were no indications that the birds regularly spent long periods sitting on the sea surface. Seawater immersion counts may, therefore, largely reflect feeding activity. Variables which made significant contributions as main effects to GLMMs of seawater immersion frequency were interval type and migration phase (analysis of deviance:  $\chi^2 > 58.8$ ,  $df = 1, 3$ ;  $p < 0.001$ ), and geolocation status (moving or within stationary periods;  $\chi^2 = 4.2$ ,  $df = 1$ ,  $p = 0.04$ ). Conversely, year group, mean wind speed and chl *a* concentrations were significant only in interactions and not as main effects ( $p > 0.2$ ; Table S2). Mean seawater immersion frequency was lower at night compared to during the day at all migration phases (Fig. 4a; least-squares mean pairwise contrasts at each phase,  $|t| > 17.6$ ,  $df = 9601$ ,  $p < 0.001$ ), and at night did not differ between phases ( $p > 0.27$  for all contrasts). Conversely, in the daytime, mean seawater

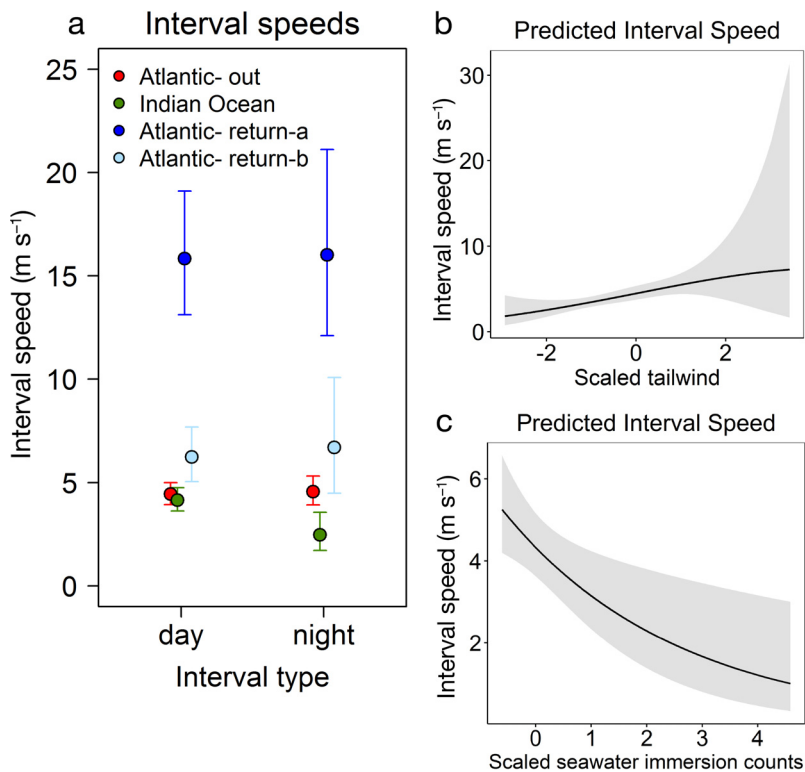


Fig. 3. (a) Mean interval speeds (error bars: 95 % CI) by day and night, corrected with respect to tailwind and seawater immersion frequency for day and night intervals; (b) variation in mean interval speed by tailwind, corrected for immersion frequency, and day/night; (c) variation in interval speeds by immersion frequency, during Arctic tern migration phases from fitted GLMM. Grey shading: 95 % confidence range. All data with interval speeds  $> 0$  and with individual birds as random effects; model details in Table S1

immersion frequencies differed ( $|t| > 5.5$ ,  $df = 9601$ ,  $p < 0.001$ ) between all phases except for the Indian Ocean and the first part, Return-a, of return migration ( $p = 0.37$ ; Fig. 4a); daytime mean seawater immersion frequencies were highest during the last phase of return migration and lowest during the Atlantic outward phase (Fig. 4a).

Seawater immersion frequencies during the day were higher for stationary period geolocation intervals than movement intervals ( $t = -7.5$ ,  $df = 9601$ ,  $p < 0.001$ ; Fig. 4a); there was also a similar albeit smaller effect at night ( $t = -2.78$ ,  $df = 9601$ ,  $p < 0.01$ ; Fig. 4a). With respect to migration phase, daytime immersion frequencies were higher in stationary-period geolocations intervals than in movement periods ( $|t| > 3.8$ ,  $df = 9601$ ,  $p < 0.001$ ) for all phases except for the first part of return migration where the reverse was the case ( $t = 2.31$ ,  $p = 0.021$ ). Mean seawater immersion frequencies were affected by wind conditions and decreased in relation to mean wind speed (Fig. 4b, upper graph) but, overall, varied little in relation to chl *a* (Fig. 4b, lower graph). Indeed, chl *a* concentrations at bird locations differed between phases and



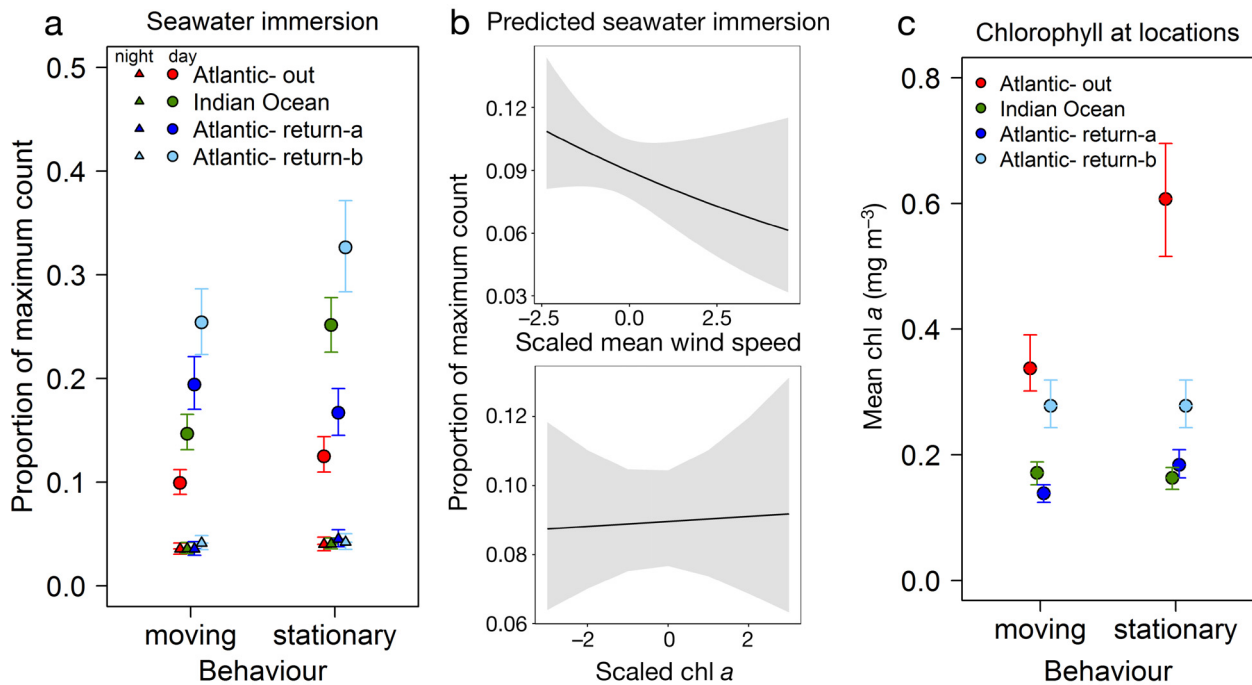


Fig. 4. Mean seawater immersion frequency (ordinate: proportion of maximum count) during Arctic tern migration phases from fitted GLMM (a) by behaviour (moving/stationary periods) during day and night intervals; (b) upper graph: in relation to mean wind speed; lower graph: in relation to chl *a* concentrations (mean within 50 km radius) at geolocations; (c) by variation in chl *a* concentrations at geolocations (mean within 50 km radius) within each phase from GLMM with chl *a* as dependent variable. Error bars: 95 % CI; grey shading: 95 % confidence range. All data were used for GLMMs with individual birds as random effects. Model details in Tables S2 (seawater immersion) & S3 (chl *a*)

were highest during southward migration through the Atlantic and lowest in the Indian Ocean and Return-a phases (Fig. 4c, Table S3). Within migration phases, chl *a* concentrations were higher at stationary-period geolocations than movement periods only in the Atlantic and first part of the return migration (Fig. 4c;  $z > 8$ , df = asymptotic,  $p < 0.001$ , otherwise:  $p > 0.1$ ).

### 3.4. Consistency in migration routes and the effects of wind

For repeat birds, we compared trajectories in the Atlantic (outward and return) and Indian Ocean phases each year (Text S1, Figs. S3 & S4). Overall, for the Atlantic migration phases, trajectories for repeat birds were more similar than random pairwise comparisons (permutation Welch 2-sample *t*-test, 2-tailed, unequal variance, 10 000 Monte Carlo simulations,  $p = 0.01$  and  $p = 0.034$  for outward and return, respectively), but this was not the case for the Indian Ocean phase ( $p = 0.56$ ; Text S1). However, by subsections in the Atlantic phases representing the Hadley and mid-latitude cells of global atmospheric circulation (Fig. 2), repeat trajectories were only similar in the first section for the outward phase ( $p =$

0.002; other sections:  $p > 0.3$ ) and the last section for the return phase (latitudes 30° N to 50° N, Text S1,  $p = 0.015$ ; other sections:  $p \geq 0.18$ ). This suggests that the overall similarities of trajectories of individuals in different years for the Atlantic migration phases were biased by movement from or towards the breeding colony as a point source. Comparisons of *u* and *v* wind vectors and trajectory differences indicated that, as might be predicted, wind strength for these component vectors contributed to differences in migration trajectories between years (Text S1, Fig. S4, Table S4). Furthermore, with respect to crossing the Gulf of Guinea to the Angolan/Namibian coast directly or via a coastal route from Gabon southward, 8 of the 10 repeat birds took the same route in both years, but this proportion was not statistically significant (exact binomial test,  $p = 0.11$ ).

### 3.5. Foraging locations during migration

We asked whether potential Arctic tern foraging locations were associated with fronts in SST, SSH and chl *a*. Means for the 3 front variables were higher in stationary than in moving periods in all migratory phases, except for the Indian Ocean phase where

there was no discrimination in SSH, SST and chl *a* gradients between moving or stationary behavioural states (Fig. 5, Table S5). However, discrimination in mean front intensities between these behavioural states within the latter part of return migration, Return-b, was weak. The Indian Ocean phase had higher SSH gradients at geolocations overall and, as with chl *a* concentrations (Fig. 4), low chl *a* mean front intensities compared to other migration phases (Fig. 5).

In outward migration through the Atlantic, geolocations within stationary periods were associated with coastal upwelling systems characterised by SSH, SST and chl *a* fronts. Stationary-period geolocations in August were often within the coastal Canary Current (CC) and Gulf of Guinea (GC) large marine ecosystems (LME), and then in September further south in the BCLME and Agulhas leakage/ring upwellings along the west coast of southern Africa (Fig. 6, see annotations on Fig. 7c; Fig. S5). Once birds had rounded Cape Agulhas in late September–early October, stationary-period geolocations were associated with the marked SSH, SST and chl *a* fronts of the Agulhas Current (AC) and Agulhas Retroflection as it turns to form the eastward-flowing Agulhas Return Current (ARC). Stationary-period geolocations were also associated with fronts outside conventional ACLME limits (Figs. 6, 7, S5 & S6).

Within the Indian Ocean, once birds had moved beyond the Agulhas Retroflection and ARC (Figs. 7 &

S5), it was difficult to associate geolocations with particular oceanographic features. Latitudinally, most stationary-period geolocations were located between the eastward-flowing South Indian Counter Current (SICC) and the ARC which flows eastwards along the northern boundary of the Kerguelan Plateau (Fig. 7). These ocean areas were characterised by mesoscale (20–200 km) SSH and SST fronts to varying extents (Figs. 7 & S6). There was a noticeable concentration of stationary-period locations in areas around Îles Amsterdam and Saint Paul (Fig. 7). From bathymetric data, stationary-period geolocations were less likely to occur over the surface of deep ocean basins (deeper than –3000 m, binomial GLMM,  $z = 3.4$ ; 4275 observations, 49 groups;  $p < 0.001$ ; Figs. 7b & S7).

On return migration, geolocations within stationary periods tended to be associated with the Agulhas Retroflection and Agulhas leakage currents at the start of migration by birds in the 2015 group, but were further west and less focused for the 2017 group (Fig. 8a,b). This difference was maintained for the first part of return migration north through the Atlantic, with birds in the 2017 group taking a more central trajectory but then reorientating towards the Cape Verde archipelago; it is possible that these more-westerly longitudes for the 2017 group (Fig. 8c) were a consequence of lighter westerly winds in this stage of return migration in April 2018 (Fig. 8d). Stationary-period geolocations were sparse during this first

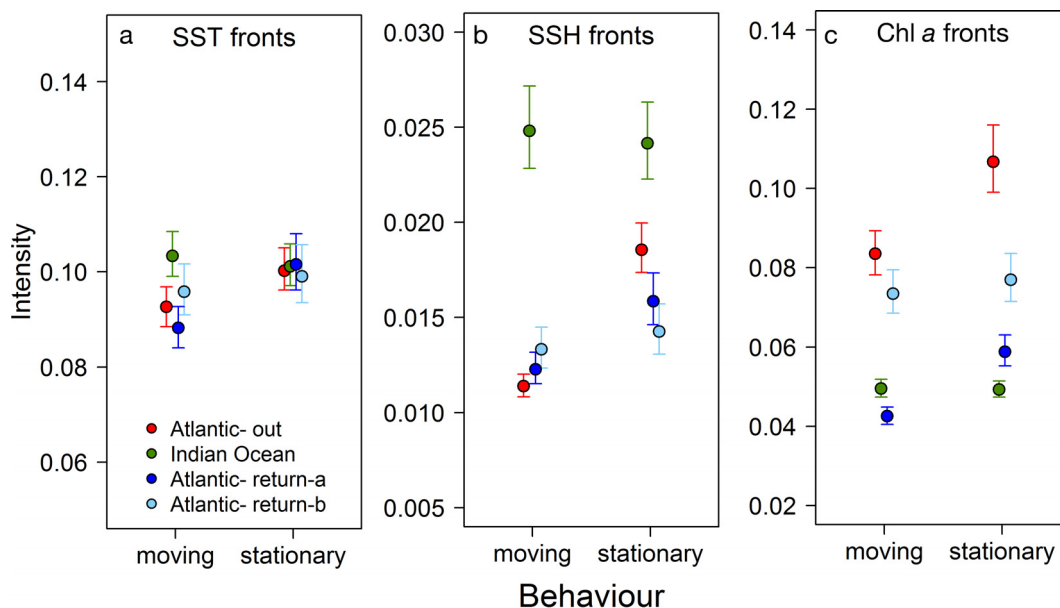


Fig. 5. Oceanography at geolocations with respect to mean fronts (gradient intensity) of (a) sea surface temperature (SST), (b) sea surface height anomalies (SSH) and (c) chl *a* concentrations, classified by behaviour (moving/stationary) for each migration phase of Arctic terns. Ordinate axes: rates of change; error bars: 95 % CI. Means are derived from GLMMs with individual birds as random effects; model details in Table S5

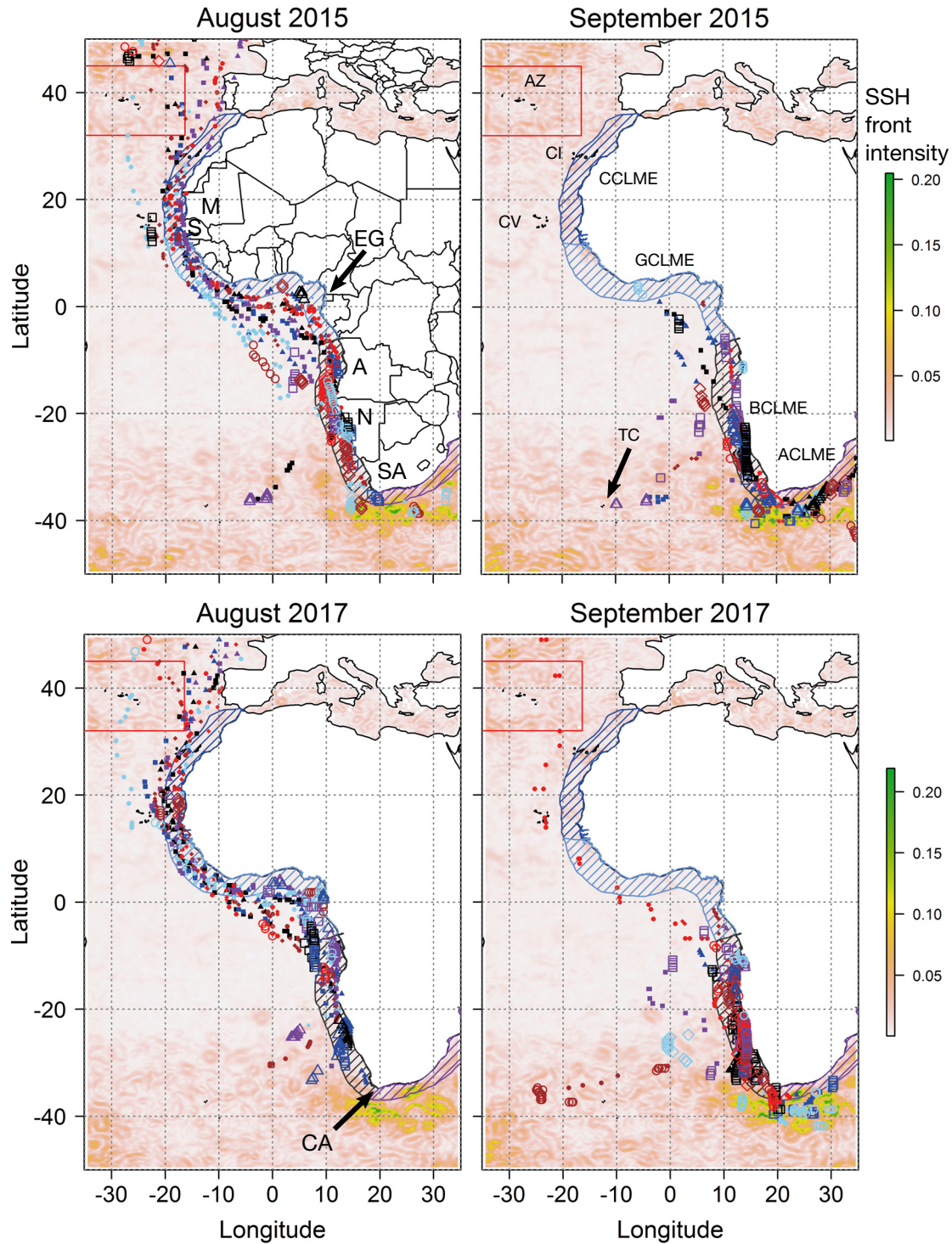


Fig. 6. SSH-gradient fronts for the Atlantic outward migration phase for August and September in both years of Arctic tern tagging. Coloured points are geolocations, with same colour and shape used for each individual bird; small, filled symbols: geolocations within movement phases; and large open symbols: stationary-period locations for the same (colour and shape) individuals. Red box in upper left of each map: Azores Confluence Zone, after Caldeira & Reis (2017). Hatched areas along west African coastline: Canary Current LME (CCLME, blue), Guinea Current LME (GCLME, light blue), Benguela Current LME (BCLME, dark green) and Agulhas Current LME (ACLME, purple). Plots for geolocations in relation to SST and chl *a* fronts are in Fig. S5. Spatial polygons for LMEs were from <https://www.marinerregions.org>. LME: large marine ecosystem; M: Mauritania; S: Senegal; EG: Equatorial Guinea; A: Angola; N: Namibia; SA: South Africa; AZ: Azores; CI: Canary Islands; CV: Cape Verde Islands; TC: Tristan da C nha; CA: Cape Agulhas



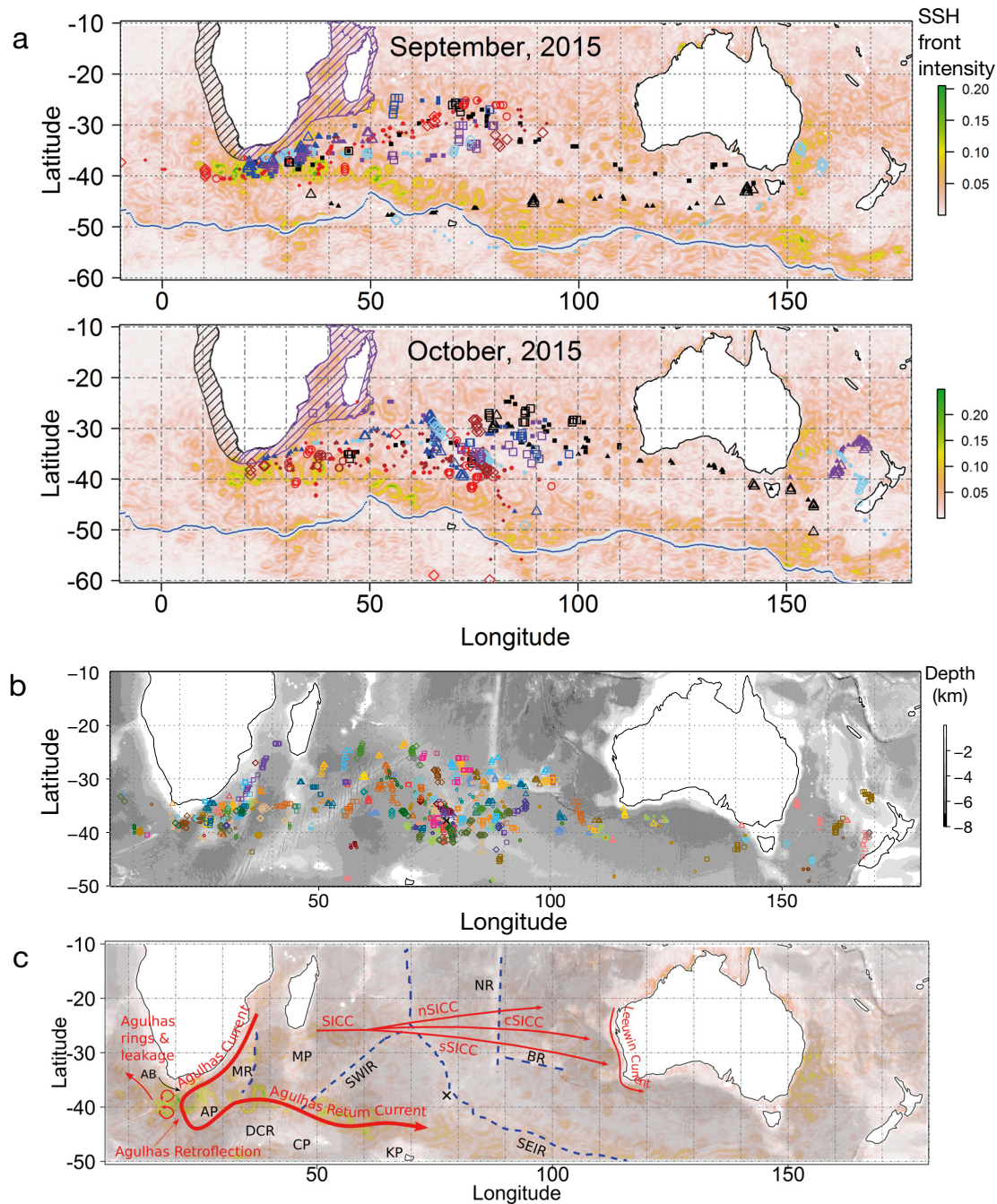


Fig. 7. (a) SSH-gradient fronts for the Indian Ocean phase for September and October 2015. Coloured points: geolocations for Arctic terns tagged in 2015 as in Fig. 6. Blue dots forming a line (grey: 95% confidence range): mean location of Antarctic Polar Front in October and November each year for 2002–2013 using data of Freeman & Lovenduski (2016). Similar plots for birds tagged in 2017 and for SST and chl *a* are in Fig. S6. Geolocations were generally north of the Subtropical Front (approximately at latitude  $-40^\circ$ ) and within the subtropical zone of the Indian Ocean (Belkin & Gordon 1996, Jaeger & Cherel 2011). (b) Stationary-period geolocations for all birds in 2015 and 2017 (open, coloured symbols with the colour/symbol shape specific to each individual) plotted on bathymetry data for the Indian Ocean (depth scale to the right: depths  $<1000$  m are in white with land separated from continental shelves by the coastline in black). (c) Bathymetric data overlaid onto SSH-gradient front plot (as in panel a) with diagrammatic representations of ocean features. Red lines: ocean current systems (Menezes et al. 2014, Castellanos et al. 2019, Civel-Mazens et al. 2021), including South Indian Counter Current (SICC), split into southern, central and northern streams (s, c and n, respectively, after Menezes et al. 2014). Bathymetric features of subsea ridges (blue dashed lines) and plateaux: AB: Agulhas Bank; AP: Agulhas Plateau; MR: Mozambique Ridge; DCR: Del Cão Rise; MP: Madagascar Plateau; CP: Crozet Plateau; SWIR: Southwest Indian Ridge; KP: Kerguelan Plateau; NR: Ninetyeast Ridge; SEIR: Southeast Indian Ridge; BR: Broken Ridge. Black cross on (b,c): Île Amsterdam (longitude 77.55, latitude  $-37.8$ )



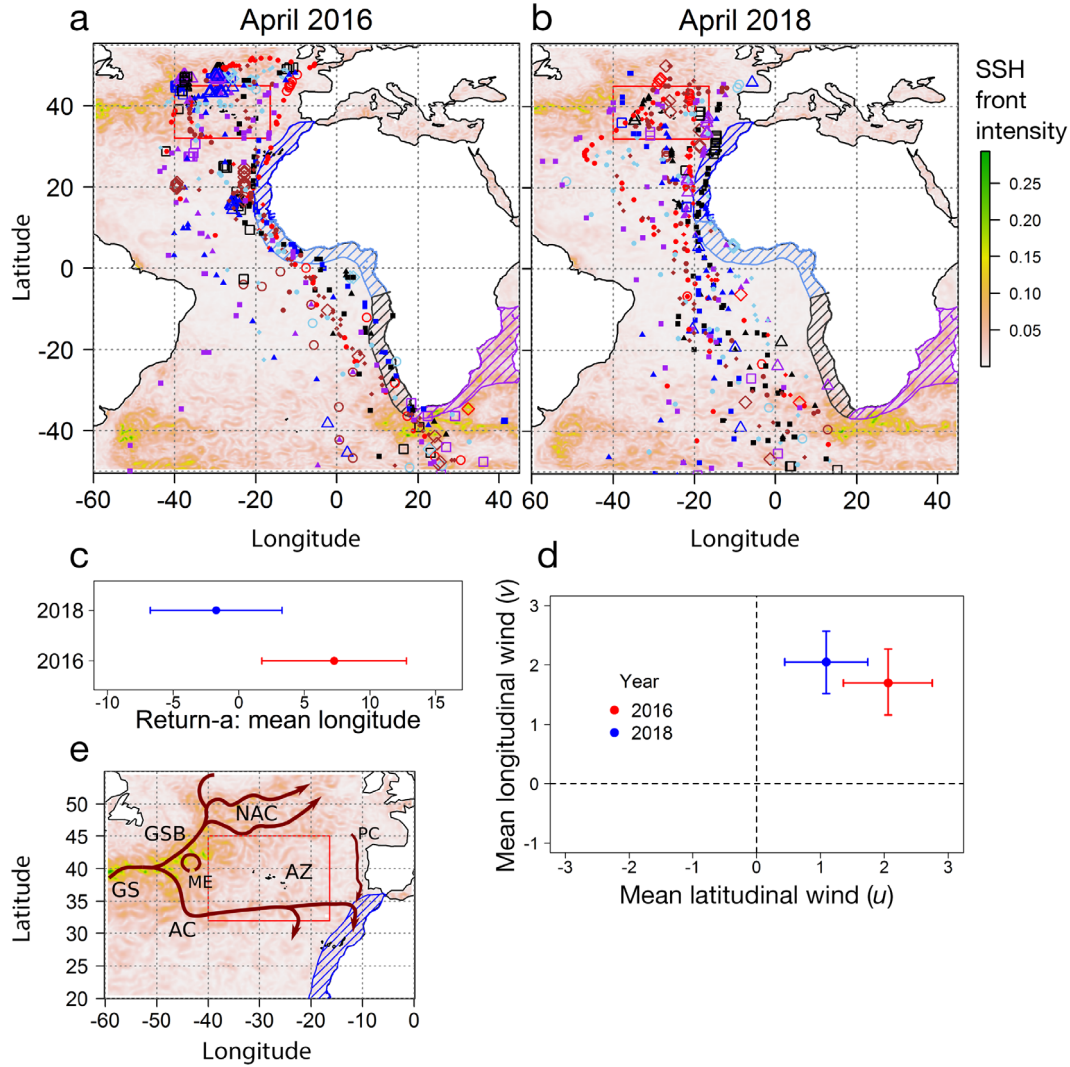


Fig. 8. (a,b) SSH-gradient fronts for Arctic tern Atlantic Ocean return phases (Return-a and Return-b) for April in the year after tagging; coloured points and SST/chl *a* plots are as in Fig. 6. Hatched areas are LMEs as in Fig. 6. (c) Mean (error bars: 95 % CI) longitudes for the Return-a phase in each year. RLMM, longitudes by latitude with year group as additive effect. (d) Mean (error bars: 95 % CI) *u* and *v* wind vectors along Return-a trajectories by year group; RLMM, wind vectors by latitude (3<sup>rd</sup>-order polynomial term) with year group as full interaction. (e) Diagrammatic detail of current systems in the North Atlantic based on Holliday et al. (2020): GS: Gulf Stream; GSB: Gulf Stream Bifurcations; AC: Azores Current; ME: Mann Eddy; NAC: North Atlantic Current; AZ: Azores; PC: Portugal Current. Red box: Azores Confluence Zone (Caldeira & Reis 2017); blue-hatched area: CCLME. Plots on SST and chl *a* data are in Fig. S8

return migration phase but more prevalent from the Cape Verde archipelago northwards. In the Cape Verde area, stationary-period geolocations were further west than the coastal Mauritania-Senegalese component of the CCLME upwelling system used by some birds on outward migration in 2017. Further north, stationary-period geolocations were frequently within areas of high SSH anomaly gradients associated with the current and eddy systems arising from bifurcations of the Gulf Stream into the North Atlantic (NAC) and Azores Currents (Figs. 8e & S8).

### 3.6. Foraging locations by repeat individuals in different years

For all migration phases, few of the repeat birds had stationary periods in the same locations in different years (Fig. 9). However, this is a question of scale; in the Atlantic outward phase, repeat individuals used the upwelling systems of the GCLME, BCLME and ACLME in the subsequent year, but in different locations. One repeat bird used the Tasman Sea between New Zealand and Australia in both years.

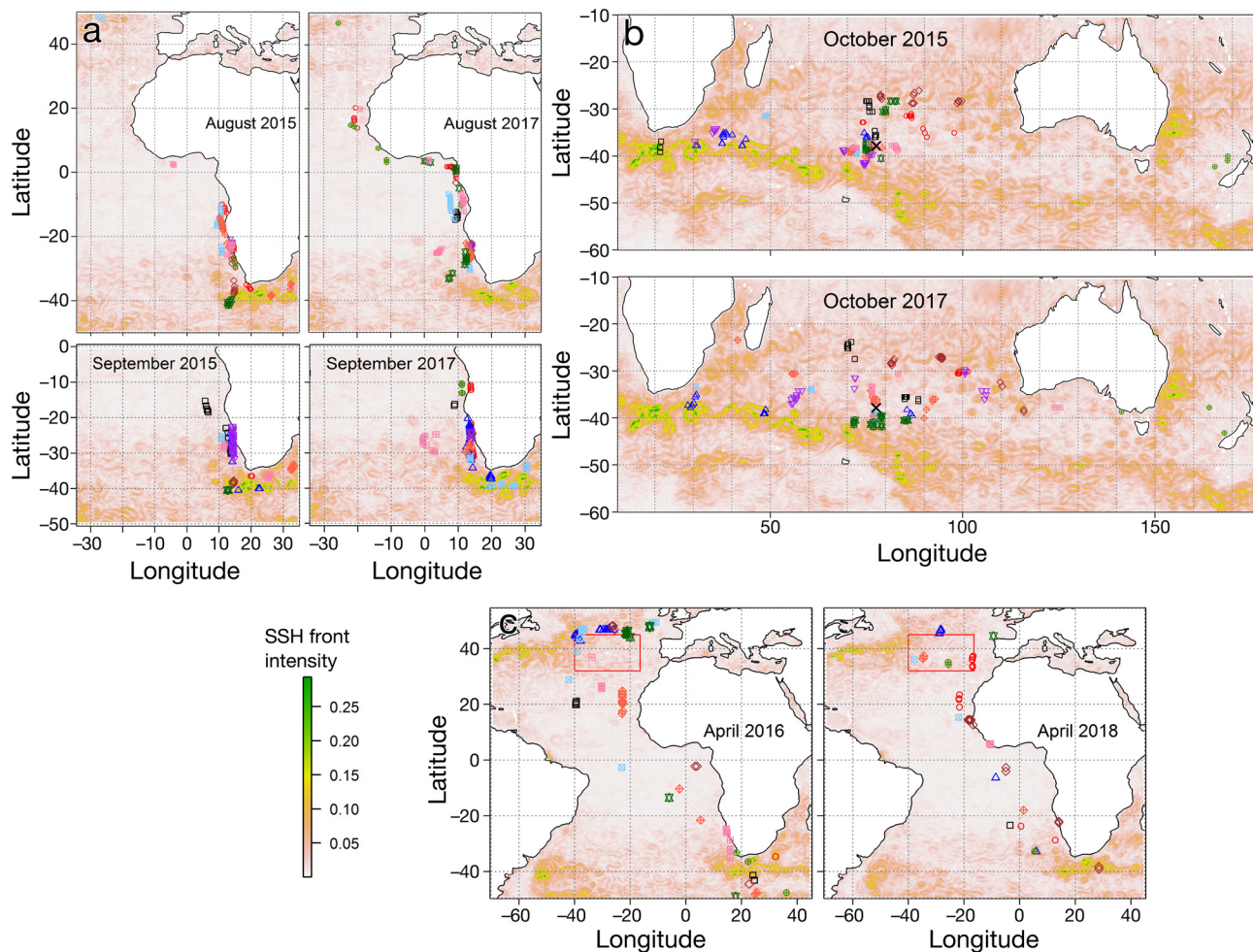


Fig. 9. Arctic tern geolocations falling within stationary periods for the same individuals tagged in 2015 and 2017; the same symbol shape (all are unfilled symbols) and colour used for the same individuals in 2015 and 2017. Geolocations plotted onto SSH anomaly gradient data for (a) Atlantic outward phase in August and September, (b) Indian Ocean phase in October and (c) return migration in April for each year

## 4. DISCUSSION

### 4.1. Fly-forage

The lack of evidence for substantial periods on the water at night at any migration phase suggests that the birds remained on the wing, at least during the long Indian Ocean traverse where birds were far from land. During this phase, birds would have to sleep while in flight (Jaeger et al. 2017, Rattenborg 2017), unless turtles, boats or ocean debris provide opportunities for settling (Haney 1986, Pitman 1993). Although some seabird species can forage at night (Phalan et al. 2007, Kokubun et al. 2015), for Arctic terns the seawater immersion data imply that plunge-dive foraging is largely confined to daylight hours. Nevertheless, contact dip-feeding at night, which would not involve immersion other than contact be-

tween the bill and water (Ashmole & Ashmole 1967), cannot be excluded and has been observed at night in sooty tern *Sterna fuscata* (Gould 1967).

The statistical inference method used for light-level analysis is based partly on hidden Markov models of animal movement (Rakhimberdiev et al. 2015) and allows classification of geolocation intervals into 'moving' and 'stationary' from the time of entry to, and exit from, stationary periods. The higher daytime seawater immersion counts in stationary-period geolocation intervals, except for the first part of the return migration, implies a migration strategy with periods of directed movement interrupted by periods of a few days foraging within a more restricted range. The relatively high daytime immersion counts during the first stage of return migration along direct great circle routes, particularly in movement geolocation periods, suggests a fly-forage mode where high

movement speeds were sustained by foraging along the way. During outward migration to the non-breeding areas, the routes taken were not direct and may be determined by behavioural strategies to maximise potential foraging opportunities (Hromádková et al. 2020). Foraging behaviour varied according to different migration stages, and this adaptability is consistent with differences, at a small spatial scale, of stationary-period locations of repeat birds between years.

#### 4.2. Foraging areas during migration

The diet of Arctic terns in the Antarctic is biased towards krill (Redfern & Bevan 2020b), but little is known of their diet and foraging during migration. This is important because their migratory foraging resources will be significant targets for future conservation. Upwelling systems are used by Arctic terns on migration (McKnight et al. 2013) and stationary-period geolocations on the Atlantic outward journey of Arctic terns from the Farne Islands were within Atlantic eastern boundary upwelling systems. In this migration phase, chl *a* concentrations and front intensities at geolocations were higher than other phases, with good discrimination between moving and stationary-period geolocations. The CCLME is complex, with permanent as well as seasonal elements, but GCLME upwelling systems reach peak intensity in July–September (Roy 1995), and the departure of Arctic terns from the British Isles in early August will enable them to exploit GCLME resources at the best time. Further south, the Angola upwellings, a component of the highly productive BCLME upwellings complex (Hutchings et al. 2009, Shannon et al. 2020), were used by the Arctic terns on outward migration in both years. These upwelling systems have considerable marine biodiversity and are used by other seabirds, either local breeders, or migrants using them as short- or longer-term foraging areas (Duffy 1989, Grecian et al. 2016, van Bemmelen et al. 2017).

The westward movement of a few of the tagged birds away from eastern boundary upwelling systems and along the line of the Walvis Ridge towards the Tristan da C  nha archipelago could be representative of Arctic terns more widely, not just birds from the Farne Islands. The Walvis Ridge (Perez et al. 2012, Campanella et al. 2021) benefits from biological productivity transported northwest from the ACLME by anticyclonic (upwelling) eddies derived from Agulhas rings (Villar et al. 2015, Laxenaire et al. 2018). This part of the South Atlantic deserves greater recognition for its high biological productivity and

importance to migratory seabirds in general (Gilg et al. 2013, van Bemmelen et al. 2017, Visalli et al. 2020).

In the Indian Ocean, as the birds moved away from the Agulhas Current system, most remained within the central subtropical zone. Although used by plunge-diving species (Hyrenbach et al. 2007), the forage prey available to terns and other seabirds here are poorly known. In contrast to the nutrient-rich upwellings of the ACLME and adjacent waters (Vousden 2016), zoo- and phytoplankton communities of the oligotrophic central Indian Ocean are shaped by different oceanographic and biological processes (Jaspers et al. 2009, Schl  ter et al. 2011). From the geolocation data, SSH fronts in the Indian Ocean were more characteristic of Arctic tern locations than at other migration phases, with no discrimination between moving and stationary periods. Fronts in the subtropical zone are associated with seasonally varying eddy systems reaching a maximum in October (Zheng et al. 2015). Although turbulence associated with such eddies may be a physical cue to attract foraging terns (Lieber et al. 2021), the biological productivity of eddies can vary. Anticyclonic eddies moving west across the Indian Ocean transport chlorophyll and nutrients from the Leeuwin Current upwelling system off Western Australia (Dufois et al. 2014) and could support foraging Arctic terns; other foraging locations appeared to be over low-chlorophyll cyclonic (downwelling) eddy systems (Dufois et al. 2014) further south. Foraging opportunities in these cyclonic eddy systems could depend on productivity from microbial communities and the enhancement of nutrient flux by eddy–eddy interactions (Ewart et al. 2008, Sabarros et al. 2009).

Additional complexity in oceanographic processes underpinning biological productivity in the Indian Ocean is apparent from the greater frequency of foraging locations over seafloor ridges and plateaux with depths shallower than 3000 m. Ridge slopes and other bathymetric features can be important for the vertical cycling of nutrients (Tuerena et al. 2019, Vic et al. 2019), increasing the availability of pelagic marine life at the surface (Campanella et al. 2021). In this context,   les Amsterdam and Saint Paul, the only land interrupting the ca. 8000 km between South Africa and southwest Australia, were surrounded by stationary-period locations. While sightings of Arctic terns are scarce in this area (Roux & Martinez 1987), this is possibly because they are misidentified as Antarctic terns *S. vittata* (Cline et al. 1969) which breed in the area. The geolocator data evidently suggest that this region is an important foraging area for Arctic terns.



Stationary-period locations in the first part of return migration were sparsely distributed and may represent ad hoc foraging patches rather than predictable foraging areas. North of the equator, some stationary-period locations were at similar latitudes to the CCLME of Mauritania-Senegal but further offshore. These may be predictable foraging resources dependent on biological material transported west from the CCLME (Bonino et al. 2021). As with the ACLME, the importance of upwelling systems for seabird foraging can extend outside conventional coastal upwelling limits.

As the birds approached breeding latitudes, stationary-period locations were in and around the ACZ where dynamic oceanographic processes associated with Gulf Stream bifurcations (Caldeira & Reis 2017) generate the marine productivity exploited by seabirds and cetaceans (Afonso et al. 2020). Chl *a* concentrations there reach a peak in April (Caldeira & Reis 2017), suggesting that Arctic terns time their arrival to take advantage of associated foraging resources. The ACZ is, for Arctic terns, relatively close to the British Isles, and, for some birds, foraging there could contribute to regaining body condition for breeding, given suitable tailwinds for the final leg to the British Isles. This is an aspect of seabird breeding biology that requires further study.

#### 4.3. Why stage in the Indian Ocean?

Evidence from this and other studies indicates that the Indian Ocean traverse is a characteristic of Arctic terns breeding in the North Sea (Fijn et al. 2013, Alerstam et al. 2019), whereas Arctic terns breeding at higher latitudes remain largely in the Atlantic for their outward migration (Egevang et al. 2010, Hromádková et al. 2020). A key question is: Why do most Arctic terns from North Sea breeding populations migrate to the Antarctic via the Indian Ocean, rather than travelling down to the Weddell Sea directly as do birds breeding at higher latitudes? The possibility of good foraging conditions in the Indian Ocean could explain such a strategy (Alerstam et al. 2019). However, chl *a* front intensities and concentrations were lower at bird locations in the Indian Ocean compared to the Atlantic migration phase, as might be expected from the oligotrophic characteristics of the central subtropical Indian Ocean. This implies that the birds were foraging on prey which are less associated with chl *a*, as a marker of biological productivity, than at other migration phases. Given that Arctic terns spend, on average, over 40 d

in the Indian Ocean on migration, the nature of their diet and foraging strategies in the subtropical zone away from conventional upwelling systems is an important area for future research.

Fragmenting sea ice is the foraging habitat for Arctic terns in the Antarctic (Redfern & Bevan 2020b), and with a departure from North Sea breeding colonies timed to maximise foraging opportunities in Atlantic eastern-boundary upwelling systems, the extent of sea-ice melt in the Antarctic may not have progressed sufficiently to make it a viable foraging habitat if birds travelled directly there. Conversely, the time pressures of a shorter breeding season at higher and/or colder latitudes (Hedenström 2008, Killie et al. 2021), later departure (Hromádková et al. 2020), and the 2600 km further travelling distance to the Antarctic, means that high-latitude breeders can travel through the Atlantic at an appropriate speed to arrive in the Antarctic Weddell Sea when ice conditions provide good foraging. Such a direct movement strategy may not have been feasible for Arctic terns in the last ice age. During the last glacial maximum, summer ice extent in East Antarctica was relatively unaffected compared to the rest of Antarctica (Bentley 1999, Gersonde et al. 2005) and may have remained a viable wintering habitat. Therefore, the Indian Ocean migration route currently used by Arctic terns breeding at low latitudes is possibly a behaviour pattern that has survived since the last ice age. More direct movement to the Weddell Sea would have become viable as glacial retreat at the end of the Pleistocene Epoch reopened sub-Arctic and Arctic breeding habitat.

#### 4.4. Migration speed

Interval speeds in the first stage of return migration were higher than at other migration phases, and these were not a consequence of higher tailwinds. As is the case for outward migration south through the Atlantic, return migration crosses tradewind bands where tailwind support varies predictably with latitude and birds are exposed to tail winds and headwinds to similar extents. Trajectories during this stage approximated to great circle routes, the shortest distance between points but requiring constant bearing correction (Åkesson & Bianco 2016). The latter part of return migration, north from latitude 15° N, was slower, but still, in daytime at least, faster than either of the outward phases. This stage was also characterised by the highest daytime seawater immersion frequencies than other migration phases,



adding support to speculation that foraging in and around the ACZ could contribute to achieving body condition for breeding. High movement speeds during the first part of return migration and high foraging activity as birds approach breeding latitudes may be behavioural adaptations to optimise breeding success.

#### 4.5. Migration phenology

The phenology of migration is likely to depend on interactions between endogenous circannual rhythms and cues such as day length (Gwinner 1996, Visser et al. 2010, Åkesson et al. 2017), but variation in phenology between years can be influenced by a variety of factors. Without the imperative to breed, departure from the breeding area can be delayed in unfavourable weather (Redfern et al. 2021), but individual repeatability in departure date suggest that birds establish preferences for linking their departure timing to the likely availability of foraging resources along the way.

Before arrival in the Antarctic, initiation of the Indian Ocean traverse and then departure from the southern Indian Ocean differed in repeatability. As an intermediate stage, starting to cross the Indian Ocean may lack seasonal imperative and be flexible according to weather and foraging conditions. Conversely, arriving at productive foraging opportunities in different Antarctic regions at the right time will be important. Repeat birds show a preference for returning to similar Antarctic longitudes each year (Redfern & Bevan 2020b) and repeatability in timing of their movement south from the Indian Ocean may enable them to arrive at the Antarctic sea-ice margin at an appropriate time to maximise foraging opportunities as the austral spring progresses. Day length is unlikely to be a cue for initiating movements south as there was a lack of repeatability in the latitude at which this was initiated, implying that departure is initiated by endogenous circannual rhythms. Furthermore, these departure latitudes were well north of the Antarctic Polar Front, which, in this region, is influenced by bathymetry and relatively consistent in location from year to year (Freeman & Lovenduski 2016). Hence, it is perhaps unlikely that the birds will have environmental cues to predict Antarctic ice extent and adapt their departure date accordingly. Instead, evidence suggests that birds respond to variations in ice conditions as and when they encounter them further south (Redfern & Bevan 2020b). Individual preferences for the time of leaving the Indian Ocean may be based on prior experience of foraging

conditions during travel to and on arrival at their target Antarctic location.

For the return migration, delaying departure from the wintering areas may have consequences for breeding success (Redfern 2021). The lack of repeatability in return timing suggests less benefit for establishing individual preferences in migration phenology at that stage. Intra-individual flexibility in response to environmental cues to ensure timely arrival at the breeding colony may be important, as has been described for migratory songbirds on return migration (Fraser et al. 2019).

#### 4.6. Repeatability in spatial use

Our working hypothesis was that individual birds will follow a similar migration route each year. Although trajectories in the Atlantic on the outward and return migrations were similar between years, particularly when displacement as a result of variation in wind conditions was taken into account, part of the trajectory similarity within individuals between years was an inevitable consequence of navigation towards or from a specific target, the breeding area. With respect to foraging behaviour as evidenced from stationary-period geolocations, even for areas with predictable foraging opportunities such as the LMEs, individuals did not use these to the same extent, or use the same locations within them, consistently in different years. In the Indian Ocean, a phase in migration relatively independent from a breeding or wintering area target, there was no evidence for latitudinal similarities in trajectories by repeat individuals between years. Once away from the influence of the Agulhas Current, good foraging resources may be dependent on oceanographic conditions in the Indian Ocean that are less predictable or focused.

Thus, for the Arctic terns tagged in different years, there was considerable year-to-year variation in behaviour while on migration as well within their 'wintering' areas (Redfern & Bevan 2020b). Similar results have been reported for other long-lived seabirds (Brown et al. 2021) and raptors (López-López et al. 2014), and also for shorter-lived passerines (van Wijk et al. 2016). Against this background of year-to-year variability in aspects of migration behaviour, the seasonal timing of some migratory events for these species, as shown here for Arctic terns, can be relatively consistent within individuals between years. Furthermore, Arctic terns do show preference, or repeatability, with respect to their longitudes of entry into Antarctica (Redfern & Bevan 2020b). In that

sense, as suggested for lesser black-backed gulls *Larus fuscus* at a smaller spatial scale (Brown et al. 2021), individual Arctic terns have their own wintering area target, but can vary routes taken depending on environmental conditions, such as wind and foraging opportunities. That will be particularly true for the Indian Ocean, an environment likely to have less predictable foraging opportunities than Atlantic eastern boundary upwelling systems.

#### 4.7. Conclusions

During their annual cycle, Arctic terns are unique in experiencing, and being adapted to, coastal and oceanic marine environments, and polar ice in both the northern and southern hemispheres. On migration, Arctic terns are likely to remain on the wing for long periods and feed during daylight as part of a fly-forage behaviour where periods of directed movement are separated by relatively stationary periods with greater foraging activity. In this context, spatial use of the marine environment will be determined by the availability of adequate foraging resources. Most stationary-period locations were within biologically productive upwelling systems, especially during the Atlantic outward and return phases. We cannot directly measure foraging activity, prey or foraging success using geolocators, but the birds were likely to be exploiting prey resources in these areas. Elsewhere, particularly in the Indian Ocean, foraging resources used by these birds are poorly characterised. Wide-spread mesoscale oceanic eddy systems with lower and unpredictable biological productivity in the Indian Ocean, perhaps enhanced by ocean-floor topography, may require the birds to adopt greater flexibility in movement and foraging patterns than at other migration stages. Arctic terns therefore need foraging strategies to use marine environments with predictable foraging opportunities and also those where prior experience is less helpful in finding food (Jeffries et al. 2021). Further studies are needed to identify the diet, foraging techniques and foraging success of Arctic terns, and to understand the oceanographic mechanisms generating and sustaining prey availability at all stages in migration. Use of the Indian Ocean by Arctic terns from low-latitude north-west European colonies will enable them to avoid arriving at the Antarctic before foraging within fragmenting sea ice is possible, a behaviour pattern which may have survived since the last ice age. Return migration through the Atlantic was marked by high movement speeds and high foraging intensity in the

early and later stages of return, respectively, that may be driven by the need to optimise reproductive success. These results add new dimensions to our understanding of seabird migration ecology and evolution.

**Acknowledgements.** We are grateful to BBC Springwatch and Migrate Technology for the provision of geolocators in 2015, and to the Seabird Group and members of the Natural History Society of Northumbria who generously funded the geolocators used in 2017. We thank David Steel for providing the initial introduction to the BBC Springwatch team which enabled this project to get started while he was Head Ranger on the Farne Islands. We also thank the National Trust, and the Farne Islands Ranger Team on Inner Farne, subsequently led by Harriet Reid, for their support and encouragement of the study, and the Natural History Society of Northumbria for additional support, encouragement and interest in the project. Lastly, we thank the reviewers and editorial team for their comments and input which greatly improved the final manuscript.

#### LITERATURE CITED

- ✦ Afonso P, Fontes J, Giacomello E, Magalhães MC and others (2020) The Azores: a mid-Atlantic hotspot for marine megafauna research and conservation. *Front Mar Sci* 6:826
- ✦ Åkesson S, Bianco G (2016) Assessing vector navigation in long-distance migrating birds. *Behav Ecol* 27:865–875
- ✦ Åkesson S, Hedenström A (2007) How migrants get there: migratory performance and orientation. *Bioscience* 57: 123–133
- ✦ Åkesson S, Helm B (2020) Endogenous programs and flexibility in bird migration. *Front Ecol Evol* 8:78
- ✦ Åkesson S, Ilieva M, Karagicheva J, Rakhimberdiev E, Tomotani B, Helm B (2017) Timing avian long-distance migration: from internal clock mechanisms to global flights. *Philos Trans R Soc B* 372:20160252
- ✦ Alerstam T, Bäckman J, Grönroos J, Olofsson P, Strandberg R (2019) Hypotheses and tracking results about the longest migration: the case of the Arctic tern. *Ecol Evol* 9: 9511–9531
- Ashmole NP, Ashmole MJ (1967) Comparative feeding ecology of sea birds of a tropical oceanic island. *Bull Peabody Mus Nat Hist* 40:1–131
- ✦ Bates D, Mächler M, Bolker B, Walker S (2015) Fitting linear mixed-effects models using lme4. *J Stat Softw* 67:1–48
- ✦ Belkin IM (2021) Review: remote sensing of ocean fronts in marine ecology and fisheries. *Remote Sens* 13:883
- ✦ Belkin IM, Gordon AL (1996) Southern Ocean fronts from the Greenwich meridian to Tasmania. *J Geophys Res Oceans* 101:3675–3696
- ✦ Belkin IM, O'Reilly JE (2009) An algorithm for oceanic front detection in chlorophyll and SST satellite imagery. *J Mar Syst* 78:319–326
- ✦ Bentley MJ (1999) Volume of Antarctic ice at the Last Glacial Maximum, and its impact on global sea level change. *Quat Sci Rev* 18:1569–1595
- ✦ Bonino G, Lovecchio E, Gruber N, Münnich M, Masina S, Iovino D (2021) Drivers and impact of the seasonal variability of the organic carbon offshore transport in the Canary upwelling system. *Biogeosciences* 18:2429–2448

- Brooks M, Kristensen K, van Benthem K, Magnusson A and others (2017) glmmTMB balances speed and flexibility among packages for zero-inflated generalized linear mixed modeling. *R J* 9:378–400
- Brown JM, van Loon EE, Bouten W, Camphuysen KCJ and others (2021) Long-distance migrants vary migratory behaviour as much as short-distance migrants: an individual-level comparison from a seabird species with diverse migration strategies. *J Anim Ecol* 90:1058–1070
- Butler PJ (2016) The physiological basis of bird flight. *Philos Trans R Soc B* 371:20150384
- Caldeira RMA, Reis JC (2017) The Azores confluence zone. *Front Mar Sci* 4:37
- Campanella F, Collins MA, Young EF, Laptikhovsky V, Whomersley P, van der Kooij J (2021) First insight of meso- and benthic-pelagic fish dynamics around remote seamounts in the South Atlantic Ocean. *Front Mar Sci* 8:693
- Castellanos P, Olmedo E, Pelegrí JL, Turiel A, Campos EJD (2019) Seasonal variability of retroflection structures and transports in the Atlantic Ocean as inferred from satellite-derived salinity maps. *Remote Sens* 11:802
- Civel-Mazens M, Crosta X, Cortese G, Michel E and others (2021) Impact of the Agulhas Return Current on the oceanography of the Kerguelen Plateau region, Southern Ocean, over the last 40 kyrs. *Quat Sci Rev* 251:106711
- Cline DR, Siniff DB, Erickson AW (1969) Summer birds of the pack ice in the Weddell Sea, Antarctica. *Auk* 86:701–716
- Duffy DC (1989) Seabird foraging aggregations: a comparison of two southern upwellings. *Colon Waterbirds* 12:164–175
- Duffy DC, Mcknight A, Irons DB (2014) Trans-Andean passage of migrating Arctic terns over Patagonia. *Mar Ornithol* 41:155–159
- Dufois F, Hardman-Mountford NJ, Greenwood J, Richardson AJ, Feng M, Herbette S, Matear R (2014) Impact of eddies on surface chlorophyll in the South Indian Ocean. *J Geophys Res Oceans* 119:8061–8077
- Egevang C, Stenhouse IJ, Phillips RA, Petersen A, Fox JW, Silk JRD (2010) Tracking of Arctic terns *Sterna paradisaea* reveals longest animal migration. *Proc Natl Acad Sci USA* 107:2078–2081
- Ewart CS, Meyers MK, Wallner ER, McGillicuddy DJ, Carlson CA (2008) Microbial dynamics in cyclonic and anticyclonic mode-water eddies in the northwestern Sargasso Sea. *Deep Sea Res II* 55:1334–1347
- Fayet AL, Freeman R, Anker-Nilssen T, Diamond A and others (2017) Ocean-wide drivers of migration strategies and their influence on population breeding performance in a declining seabird. *Curr Biol* 27:3871–3878.e3
- Fernández-López J, Schliep K (2019) rWind: download, edit and include wind data in ecological and evolutionary analysis. *Ecography* 42:804–810
- Fijn RC, Hiemstra D, Phillips RA, van der Winden J (2013) Arctic terns *Sterna paradisaea* from the Netherlands migrate record distances across three oceans to Wilkes Land, East Antarctica. *Ardea* 101:3–12
- Fox J, Weisberg S (2011) An R companion to applied regression, 3rd edn. Sage Publications, Thousand Oaks, CA
- Fraser KC, Shave A, de Greef E, Siegrist J, Garroway CJ (2019) Individual variability in migration timing can explain long-term, population-level advances in a songbird. *Front Ecol Evol* 7:324
- Freeman NM, Lovenduski NS (2016) Mapping the Antarctic Polar Front: weekly realizations from 2002 to 2014. *Earth Syst Sci Data* 8:191–198
- GEBCO Bathymetric Compilation Group (2021) The GEBCO 2021 Grid—a continuous terrain model of the global oceans and land. NERC EDS British Oceanographic Data Centre NOC
- Gersonde R, Crosta X, Abelman A, Armand L (2005) Sea-surface temperature and sea ice distribution of the Southern Ocean at the EPILOG Last Glacial Maximum—a circum-Antarctic view based on siliceous microfossil records. *Quat Sci Rev* 24:869–896
- Gilg O, Moe B, Hanssen SA, Schmidt NM and others (2013) Trans-equatorial migration routes, staging sites and wintering areas of a high-Arctic avian predator: the long-tailed skua (*Stercorarius longicaudus*). *PLOS ONE* 8:e64614
- Goerg GM (2011) Lambert W random variables—a new family of generalized skewed distributions with applications to risk estimation. *Ann Appl Stat* 5:2197–2230
- Goerg GM (2020) LambertW: probabilistic models to analyze and Gaussianize heavy-tailed, skewed data. R package version 0.6.6. <https://cran.r-project.org/package=LambertW>
- Gould PJ (1967) Nocturnal feeding of *Sterna fuscata* and *Puffinus pacificus*. *Condor* 69:529
- Grecian WJ, Witt MJ, Attrill MJ, Bearhop S and others (2016) Seabird diversity hotspot linked to ocean productivity in the Canary Current large marine ecosystem. *Biol Lett* 12:20160024
- Gwinner E (1996) Circadian and circannual programmes in avian migration. *J Exp Biol* 199:39–48
- Haney JC (1986) Seabird patchiness in tropical oceanic waters: the influence of Sargassum 'reefs'. *Auk* 103:141–151
- Hedenström A (2008) Adaptations to migration in birds: behavioural strategies, morphology and scaling effects. *Philos Trans R Soc B* 363:287–299
- Hijmans RJ, Williams E, Vennes C (2019) geosphere: spherical trigonometry. R package version 1.5-10. <https://cran.r-project.org/package=geosphere>
- Holliday NP, Bersch M, Berx B, Chafik L and others (2020) Ocean circulation causes the largest freshening event for 120 years in eastern subpolar North Atlantic. *Nat Commun* 11:585
- Hromádková T, Pavel V, Flousek J, Briedis M (2020) Seasonally specific responses to wind patterns and ocean productivity facilitate the longest animal migration on Earth. *Mar Ecol Prog Ser* 638:1–12
- Hutchings L, van der Lingen CD, Shannon LJ, Crawford RJM and others (2009) The Benguela Current: an ecosystem of four components. *Prog Oceanogr* 83:15–32
- Hyrenbach KD, Veit RR, Weimerskirch H, Metzl N, Hunt GL (2007) Community structure across a large-scale ocean productivity gradient: marine bird assemblages of the Southern Indian Ocean. *Deep Sea Res I* 54:1129–1145
- Jaeger A, Cherel Y (2011) Isotopic investigation of contemporary and historic changes in penguin trophic niches and carrying capacity of the Southern Indian Ocean. *PLOS ONE* 6:e16484
- Jaeger A, Feare CJ, Summers RW, Lebarbenchon C, Larose CS, Le Corre M (2017) Geolocation reveals year-round at-sea distribution and activity of a superabundant tropical seabird, the sooty tern *Onychoprion fuscatus*. *Front Mar Sci* 4:394

- ✦ Jaspers C, Nielsen TG, Carstensen J, Hopcroft RR, Møller EF (2009) Metazooplankton distribution across the Southern Indian Ocean with emphasis on the role of Larvaceans. *J Plankton Res* 31:525–540
- ✦ Jeffries PM, Patrick SC, Potts JR (2021) Be different to be better: the effect of personality on optimal foraging with incomplete knowledge. *Theor Ecol* 14:575–587
- ✦ Jones MS, Allen M, Guymer T, Saunders M (1998) Correlations between altimetric sea surface height and radiometric sea surface temperature in the South Atlantic. *J Geophys Res Oceans* 103:8073–8087
- ✦ Kemp MU, van Loon EE, Shamoun-Baranes J, Bouten W (2012) RNCEP: global weather and climate data at your fingertips. *Methods Ecol Evol* 3:65–70
- ✦ Killick R, Fearnhead P, Eckley IA (2012) Optimal detection of changepoints with a linear computational cost. *J Am Stat Assoc* 107:1590–1598
- ✦ Killie MA, Aaboe S, Isaksen K, Van Pelt W, Pedersen ÅØ, Luks B (2021) Svalbard snow and sea-ice cover: comparing satellite data, on-site measurements, and modelling results (SvalSCESIA). In: Moreno-Ibáñez M, Hagen JO, Hübner C, Lihavainen H, Zaborska A (eds) SESS report 2020. Svalbard Integrated Arctic Earth Observing System, Longyearbyen, p 220–235
- ✦ Kokubun N, Yamamoto T, Kikuchi DM, Kitaysky A, Takahashi A (2015) Nocturnal foraging by red-legged kittiwakes, a surface feeding seabird that relies on deep water prey during reproduction. *PLOS ONE* 10: e0138850
- ✦ Koller M (2016) robustlmm: an R package for robust estimation of linear mixed-effects models. *J Stat Softw* 75:1–24
- ✦ Laxenaire R, Speich S, Blanke B, Chaigneau A, Pegliasco C, Stegner A (2018) Anticyclonic eddies connecting the western boundaries of Indian and Atlantic Oceans. *J Geophys Res Oceans* 123:7651–7677
- ✦ Lenth R (2019) emmeans: estimated marginal means. R package version 1.4.1. <https://cran.r-project.org/package=emmeans>
- ✦ Lieber L, Langrock R, Nimmo-Smith WAM (2021) A bird's-eye view on turbulence: seabird foraging associations with evolving surface flow features. *Proc R Soc B* 288: 20210592
- ✦ López-López P, García-Ripollés C, Urios V (2014) Individual repeatability in timing and spatial flexibility of migration routes of trans-Saharan migratory raptors. *Curr Zool* 60: 642–652
- ✦ McKnight A, Allyn AJ, Duffy DC, Irons DB (2013) 'Stepping stone' pattern in Pacific Arctic tern migration reveals the importance of upwelling areas. *Mar Ecol Prog Ser* 491: 253–264
- ✦ Menezes VV, Phillips HE, Schiller A, Bindoff NL, Domingues CM, Vianna ML (2014) South Indian Countercurrent and associated fronts. *J Geophys Res Oceans* 119:6763–6791
- ✦ Perez JAA, dos Santos Alves E, Clark MR, Bergstad OA, Gebruk A, Cardoso IA, Rogacheva A (2012) Patterns of life on the southern Mid-Atlantic ridge: compiling what is known and addressing future research. *Oceanography* 25:16–31
- ✦ Phalan B, Phillips RA, Silk JRD, Afanasyev V and others (2007) Foraging behaviour of four albatross species by night and day. *Mar Ecol Prog Ser* 340:271–286
- ✦ Pitman RL (1993) Seabird associations with marine turtles in the eastern Pacific Ocean. *Colon Waterbirds* 16: 194–201
- R Core Team (2019) R: a language and environment for statistical computing. R Foundation for Statistical Computing, Vienna
- ✦ Rakhimberdiev E, Winkler DW, Bridge E, Seavy NE, Sheldon D, Piersma T, Saveliev A (2015) A hidden Markov model for reconstructing animal paths from solar geolocation loggers using templates for light intensity. *Mov Ecol* 3:25
- ✦ Rakhimberdiev E, Senner NR, Verhoeven MA, Winkler DW, Bouten W, Piersma T (2016) Comparing inferences of solar geolocation data against high-precision GPS data: annual movements of a double-tagged black-tailed godwit. *J Avian Biol* 47:589–596
- ✦ Rakhimberdiev E, Saveliev A, Piersma T, Karagicheva J (2017) FLIGHTR: an R package for reconstructing animal paths from solar geolocation loggers. *Methods Ecol Evol* 8:1482–1487
- ✦ Rattenborg NC (2017) Sleeping on the wing. *Interface Focus* 7:20160082
- ✦ Redfern CPF (2021) Pair bonds during the annual cycle of a long-distance migrant, the Arctic tern (*Sterna paradisaea*). *Avian Res* 12:32
- ✦ Redfern CPF, Bevan RM (2020a) Overland movement and migration phenology in relation to breeding of Arctic terns *Sterna paradisaea*. *Ibis* 162:373–380
- ✦ Redfern CPF, Bevan RM (2020b) Use of sea ice by Arctic terns *Sterna paradisaea* in Antarctica and impacts of climate change. *J Avian Biol* 51:e02318
- ✦ Redfern CPF, Kinchin-Smith D, Newton S, Morrison P, Bolton M, Piec D (2021) Upwelling systems in the migration ecology of roseate terns (*Sterna dougallii*) breeding in northwest Europe. *Ibis* 163:549–565
- Roux JP, Martinez J (1987) Rare, vagrant and introduced birds at Amsterdam and Saint Paul Islands, Southern Indian Ocean. *Cormorant* 14:3–19
- Roy C (1995) The Côte d'Ivoire and Ghana coastal upwellings dynamics and changes. In: Bard F, Koranteng KA (eds) Dynamique et usage des ressources sardinelles de l'upwelling côtier du Ghana et de la Côte d'Ivoire. ORSTOM Éditions, Paris, p 346–361
- ✦ Sabarros PS, Ménard F, Lévénéz JJ, Tew-Kai E, Ternon JF (2009) Mesoscale eddies influence distribution and aggregation patterns of micronekton in the Mozambique Channel. *Mar Ecol Prog Ser* 395:101–107
- ✦ Schlüter L, Henriksen P, Nielsen TG, Jakobsen HH (2011) Phytoplankton composition and biomass across the southern Indian Ocean. *Deep Sea Res I* 58:546–556
- ✦ Shannon LJ, Ortega-Cisneros K, Lamont T, Winker H, Crawford R, Jarre A, Coll M (2020) Exploring temporal variability in the Southern Benguela Ecosystem over the past four decades using a time-dynamic ecosystem model. *Front Mar Sci* 7:540
- ✦ Stoffel MA, Nakagawa S, Schielzeth H (2017) rptR: repeatability estimation and variance decomposition by generalized linear mixed-effects models. *Methods Ecol Evol* 8: 1639–1644
- ✦ Tuerena RE, Williams RG, Mahaffey C, Vic C and others (2019) Internal tides drive nutrient fluxes into the deep chlorophyll maximum over mid-ocean ridges. *Glob Biogeochem Cycles* 33:995–1009
- ✦ Vágási CI, Pap PL, Vincze O, Osváth G, Erritzøe J, Møller AP (2016) Morphological adaptations to migration in birds. *Evol Biol* 43:48–59
- ✦ van Bemmelen R, Moe B, Hanssen SA, Schmidt NM and others (2017) Flexibility in otherwise consistent non-



- breeding movements of a long-distance migratory seabird, the long-tailed skua. *Mar Ecol Prog Ser* 578:197–211
- ✦ van Wijk RE, Bauer S, Schaub M (2016) Repeatability of individual migration routes, wintering sites, and timing in a long-distance migrant bird. *Ecol Evol* 6:8679–8685
- ✦ Vic C, Naveira Garabato AC, Green JAM, Waterhouse AF and others (2019) Deep-ocean mixing driven by small-scale internal tides. *Nat Commun* 10:2099
- ✦ Villar E, Farrant GK, Follows M, Garczarek L and others (2015) Environmental characteristics of Agulhas rings affect interocean plankton transport. *Science* 348:1261447
- ✦ Visalli ME, Best BD, Cabral RB, Cheung WWL and others (2020) Data-driven approach for highlighting priority areas for protection in marine areas beyond national jurisdiction. *Mar Policy* 122:103927
- ✦ Visser ME, Caro SP, Van Oers K, Schaper SV, Helm B (2010) Phenology, seasonal timing and circannual rhythms: towards a unified framework. *Philos Trans R Soc B* 365:3113–3127
- Voelker G (1997) The molt cycle of the Arctic tern, with comments on ageing criteria. *J Ornithol* 68:400–412
- ✦ Vousden D (2016) Productivity and biomass assessments for supporting management of the Agulhas Current and Somali Current large marine ecosystems. *Environ Dev* 17:118–125
- ✦ Wood SN (2011) Fast stable restricted maximum likelihood and marginal likelihood estimation of semiparametric generalized linear models. *J R Stat Soc B* 73:3–36
- ✦ Woodson CB, Litvinb SY (2015) Ocean fronts drive marine fishery production and biogeochemical cycling. *Proc Natl Acad Sci USA* 112:1710–1715
- ✦ Zheng S, Du Y, Li J, Cheng X (2015) Eddy characteristics in the South Indian Ocean as inferred from surface drifters. *Ocean Sci* 11:361–371

*Editorial responsibility: Robert M. Suryan,  
Juneau, Alaska, USA*

*Reviewed by: M. Leopold, T. Diamond and 1 anonymous  
referee*

*Submitted: November 22, 2021*

*Accepted: April 1, 2022*

*Proofs received from author(s): May 23, 2022*